Fundamental Journals
IJFPS
ISSN: 2231-8186
International Journal of Fundamental Physical Sciences
Full length Research Papers
http://fundamentaljournals.org/ijfps/index.html

On The Effect of Electron-Hole Recombination in Disordered GaAs-Aa1-xALAs Multi-quantum Well Structure

Uno E. Uno, Moses E. Emetere*, Isah K.U and Umaru Ahmadu

Federal University of Technology, Minna, Nigeria P.M.B 65, Minna, Nigeria

Email: emetere@yahoo.com

(*Received Sep 2012; Published Dec 2012*)

ABSTRACT

The disordered electron-hole recombination in multi-quantum well was investigated using analytical method based on the rate equations. The results show extreme broad distribution of the recombination time which depends exponentially on the distances between the recombining excitons. The energies at each localised state shows an energy splitting between the electronic ground state and the first excited state of 0.0038eV.

Key words: Disordered structure, semiconductor, energy transition and hopping length

INTRODUCTION

All semiconductors possess a certain degree of disorder due to their alloy structure and imperfect interfaces. This order gives rise to localized state and in turn affects the optical properties of the system. Recently, recombination of electron-hole in a disordered structure (e.g. organic semiconductor (Shushin, 2011), graphene bilayer (Efimkin, Kulbachinskii, & Lozovik, 2011) e.t.c.) has been the focus of discussion because of its importance in constructing electronics device. Small disordered one-dimensional structures was the first to be investigated (Kramer & MacKinnon, 1999),it was discovered that when there is randomness, complete localization of non-interacting electrons and holes occur which initiated a further research on the interaction of electron - hole i.e. conducted at strong coulomb interaction (Leadbeater, Römer, & Schreiber, 1999) and weakly electron-hole interaction in a random potential (Kalyanasundaram & Grätzel, 1998) to produce excitons with long and short lifetime respectively. The recombination of electron-hole rate in disordered has proven to be important in photocatalytic reactions with semiconductor particles, rectification, photoconductivity and transistor behavior (Kalyanasundaram & Grätzel, 1998). The choice of $GaAs - Aa1 - x\ ALAs$ in this paper is to due to two facts. First, reawakening a new dimension into research work of the past decade and secondly is because of its potential for applications in optoelectronic devices. The effects of type II alignment in $GaAs/AlAs$ double layer structures was achieved by the appropriate choice of the $GaAs$ and $AlAs$ layers' width (Ashoori et al., 1993; Reed, 1993) and was initially grown by molecular beam epitaxy (Isu, Jiang, & Ploog, 1987; Ohya, Ishida, & Mori, 1984) and metal organic chemical vapour deposition (Ishibashi, Kidoguchi, Sugahara, & Ban, 2000). In the existing theoretical studies of disordered structures, it was assumed that electrons and holes are strongly spatially correlated in the form of excitons (Dal Don et al., 2004). This assumption is not always valid because of variation in the application of the disorder potential. This paper is an attempt to present the analytical method based on set of rate equations to determine the uncorrelated electrons and holes in quantum wells. The simulations in section three were done using source codes from Matlab and polynomial derivations.

THEORY

To enable a better environment for our work, the following theoretical assumptions were made. **1)** The disorder in quantum well of $GaAs - Aa_{1-x}AlAs$ is caused by their alloy composition and imperfect interfaces which makes it create a set of localized states than trap photo-generated charge

carriers. The carriers are captured after photo-generation. 2) The carriers can either recombine or perform a photo–assisted hopping transition to other localized states. The probabilities depend exponentially on the distance involved. The rate of recombination with localized hole at a rate is

$$\Gamma_\sigma(R) \approx \tau_o^{-1} \exp\left(-\frac{2R}{\alpha}\right) \quad (1)$$

Where τ_o depends on the particular recombination mechanism. In the case of radioactive recombination, τ_o is of the order of the exciton radioactive life time. **3)** The rate for a charge carrier to perform a non radioactive hopping transition from an occupied state i to an empty localized state j over a distance r_{ij} is determined by the Miller, Blum, Glennon, and Burton (1960).

$$\Gamma_{ij} = V_o \exp[-\frac{2r_{ij}}{\alpha} - \frac{\xi_j - \xi_I + |\xi_j - \xi_I|}{2KT} \quad (2)$$

Where ξ_j and ξ_I are the energies of states j and i respectively and V_0 is the attempt-to-escape-frequency of the $10^{12} s^{-1}$. **4)** Applying the approach of (Marshall, 2000), one divides the energy range where the localized states are distributed into a set of m energy slices with a given width and formulates the rate equation for carrier densities in those energy slices. The time of the carrier concentration n_k in slice number k is determined by the equation

$$\frac{dn_k}{dt} = \sum_{\substack{j=i \\ j\neq k}}^{m} \left(n_j \Gamma_{j\to k} - n_k \Gamma_{k\to}\right) - n_k \Gamma_\sigma \quad (3)$$

Where $\Gamma_{j\to k}$ denotes the rate of a charge carrier transition from a state in slice i to a state in slice j, and Γ_σ is the recombination rate. **5)** Considering the transition rate $T_{k\downarrow}$ from the slice k downward in energy, since the transition occurs through energy loss hopping; only the tunnelling term remains in Eq 2. Therefore, one can write the downward transition rate as;

$$T_{k\downarrow} = V_o \exp[\frac{-2R_k}{\alpha}) \quad (4)$$

Where R_k is the hopping distance determined by energy below E_k . In two dimensional cases it can be estimated as

$$R_k = \left\{\pi \sum_{i=k}^{m} (d_j - n_i(t))\right\}^{\frac{-1}{2}} \quad (5)$$

Where d_j denotes the concentration of localized states in the energy j. Using equation 4, we can derive the downward hopping rate $\Gamma_{j\to k}$ between two energy slices as a fraction of $T_{k\downarrow}$.Therefore, the downward in energy transition rates between states in two energy slices k and , $(E_k > E_j)$ can be written in the form

$$T_{k\to j} = V_o \exp\left(\frac{-2R_k}{\alpha}\right) * \frac{d_j - n_i(t)}{\sum_{i=k}^{m}[d_j - n_i(t)]} \quad (6)$$

We can also calculate the transition rate for carriers between two slices j and k upward in energy can be derived from downward transition rate

$$T_{k\to j} = T_{k\to j} \frac{d_k - n_k(t)}{d_j - n_i(t)} \exp\left(\frac{\xi_k - \xi_j}{KT}\right) \quad (7)$$

Hence, upward in energy transition, the expression becomes

$$T_{k\to j} = V_o \exp\left(\frac{-2R_k}{\alpha} - \frac{\xi_k - \xi_j}{KT}\right) * \frac{d_j - n_i(t)}{\sum_{i=k}^{m}[d_j - n_i(t)]} \quad (8)$$

6) If the concentration of charge carriers at time t is n, the recombination rate would be of the order $\Gamma_\sigma(n^{-1/2})$. The recombination rate in equation (3) can be expressed as the product of the density of filled electron state n and the probability $n\alpha^2$ from the filled hole state of a distance α from filled electron state n;

$$\Gamma_\sigma \approx \tau_o^{-1} n(t) \alpha^2 \quad (9)$$

Applying Eq3-9 we obtain the luminescence spectrum as;

$$I(\hbar\omega, t) = \alpha \int_{-\infty}^{\infty} n^{(o)}(\hbar\omega + \xi, t) n^{(k)}(\xi, t) d\xi \quad (10)$$

Where $n^{(o)}(\xi, t)$ and $n^{(k)}(\xi, t)$ denote the densities of electron and holes respectively.

SIMULATIONS OF DERIVATIONS

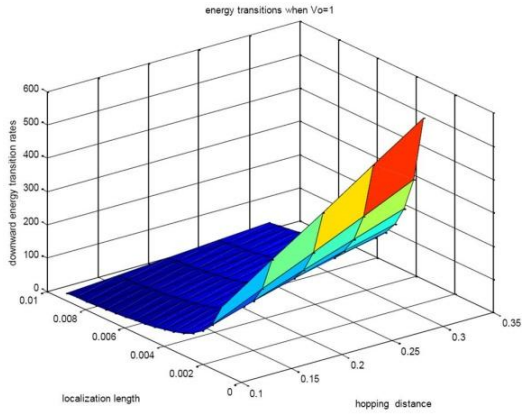

Figure.1 Effects on the downward energy transition when $V_o = 1Hz$ and $R > \alpha$ in the second Taylors expansion

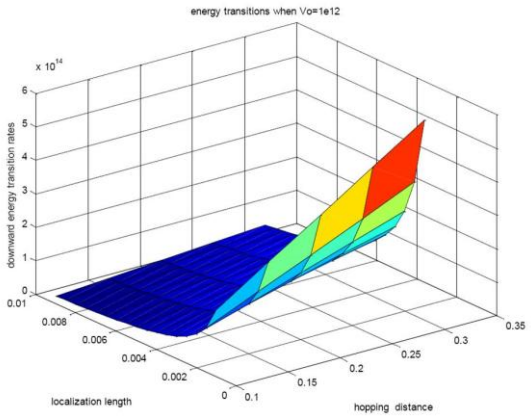

Figure.2 Effects on the downward energy transition when $V_o = 1Hz$ and $R > \alpha$ in the second Taylors expansion

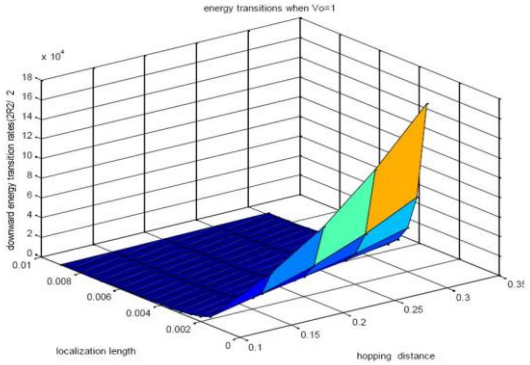

Figure.3 Effects on the downward energy transition when $V_o = 1Hz$ and $R > \alpha$ in the third Taylors expansion

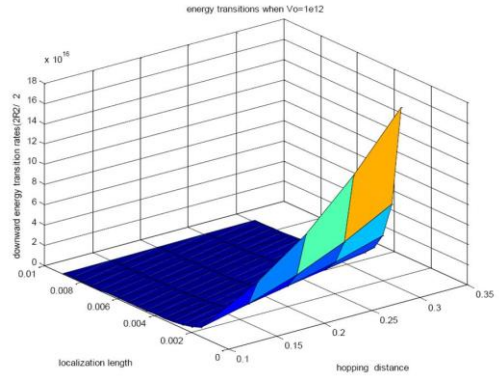

Figure.4 effects on the downward energy transition when $V_o = 1Hz$ and R>α in the third Taylors expansion

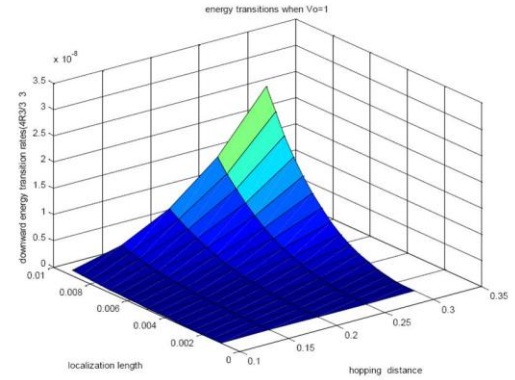

Figure.5 Effects on the downward energy transition when$V_o = 1Hz$ and R>α in the fourth Taylors expansion

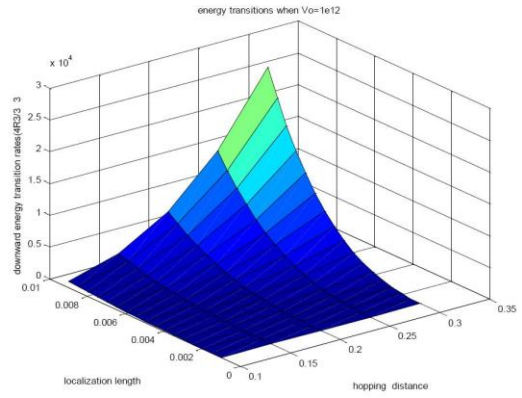

Figure.6 Effects on the downward energy transition when $V_o = 10^{12}Hz$ and $R > \alpha$ in the fourth Taylors expansion

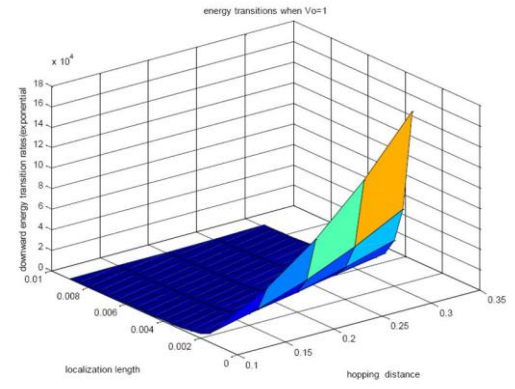

Figure.7 Effects on the downward energy transition when $V_o = 1Hz$ and $R > \alpha$ in the general Taylors expansion

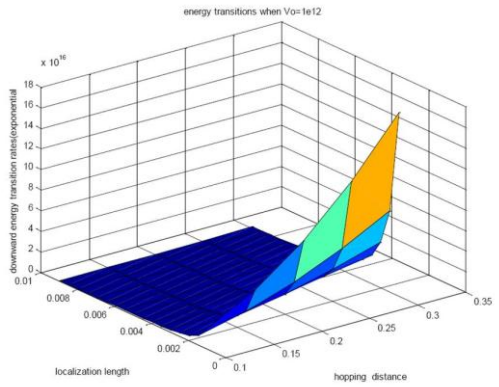

Figure.8 Effects on the downward energy transition when $V_o = 1Hz$ and $R > \alpha$ in the general Taylors expansion

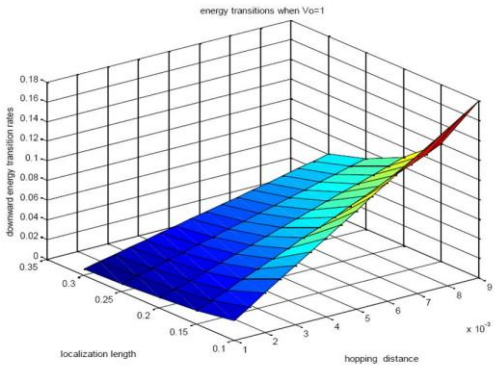

Figure.9 Downward energy transition when $V_o = 1Hz$ and $R < \alpha$ in the second Taylors expansion

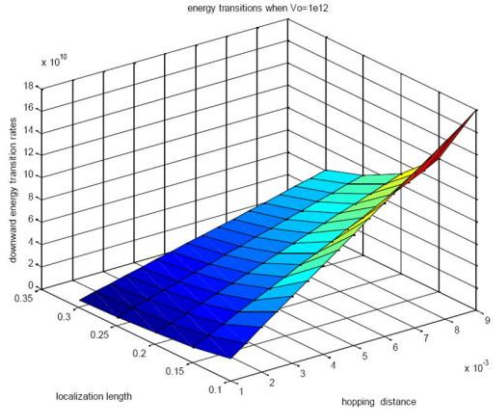

Figure.10 Effects on the downward energy transition when $V_o = 1Hz$ and $R < \alpha$ in the second Taylors expansion

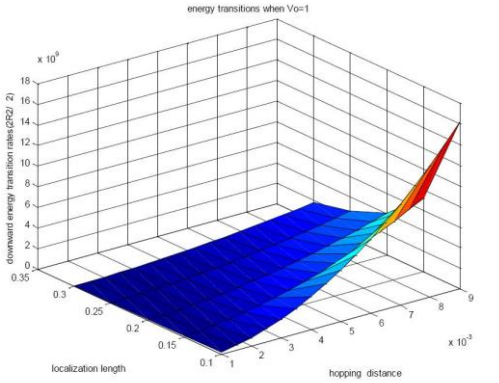

Figure.11 Downward energy transition when $V_o = 1Hz$ and $R < \alpha$ in the third Taylors expansion

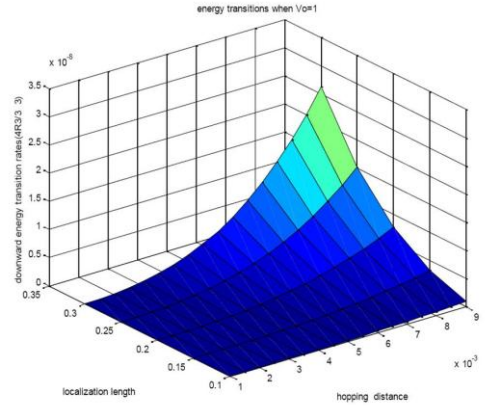

Figure.12 The downward energy transition when $V_o = 1Hz$ and $R < \alpha$ in the general Taylors expansion.

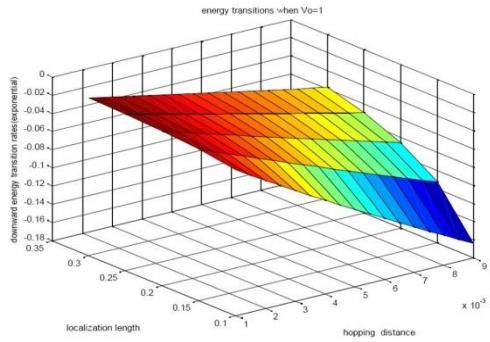

Figure.13 Downward energy transition when $V_o = 1Hz$ and $R < \alpha$ in the general Taylors expansion

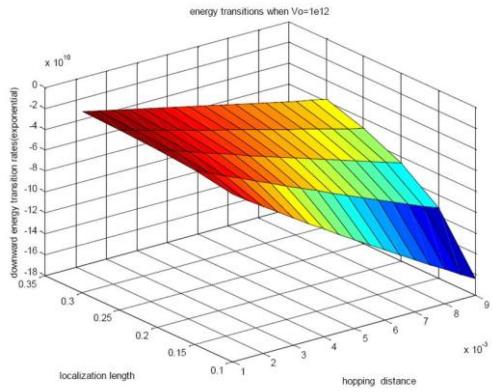

Figure.14 Downward energy transition when $V_o = 10^{12}Hz$ and $R < \alpha$ in the general Taylors expansion.

The simulations on equations (4) were carried as shown in the figure above. The Taylors expansion was applied to analyze the features of the various changes in the downward energy transitions. Figure (1) describes the effects on the downward energy transition when $V_o = 1Hz$ and $R > \alpha$ in the second Taylors expansion. Figure (2) describes the effects on the downward energy transition when $V_o = 10^{12}Hz$ and R>α in the second Taylors expansion. Figure (3) describes the effects on the downward energy transition when $V_o = 1Hz$ and $R > \alpha$ in the third Taylors expansion. Figure (4) describes the effects on the downward energy transition when $V_o = 10^{12}Hz$ and $R > \alpha$ in the third Taylors expansion. Figure (5) describes the effects on the downward energy transition when $V_o = 1Hz$ and $R > \alpha$ in the fourth Taylors expansion. Figure (6) describes the effects on the downward energy transition when $V_o = 10^{12}Hz$ and R>α in the fourth Taylors expansion. Figure (7) describes the effects on the downward energy transition when $V_o = 1Hz$ and R>α in the general Taylors expansion. Figure (8) describes the effects on the downward energy transition whenVo=10^{12}Hz and R>α in the general Taylors expansion. Figure (9) describes the effects on the downward energy transition when $V_o = 1Hz$ and R<α in the second Taylors expansion. Figure (10) describes the effects on the downward energy transition when $V_o = 1Hz$ and $R < \alpha$ in the second Taylors expansion. Figure (11) describes the effects on the downward energy transition when $V_o = 1Hz$ and $R < \alpha$ in the third Taylors expansion. Figure (12) describes the effects on the downward energy transition when$Vo = 1Hz$ and $R < \alpha$ in the fourth Taylors expansion. Figure (13) describes the effects on the downward energy transition when $V_o = 1Hz$ and R<α in the general Taylors expansion. Figure (14) describes the effects on the downward energy transition when $V_o = 10^{12}Hz$ and R<α in the general Taylors expansion. The values of the downward transition energies gotten from the figures above were assumed to be equal to the upward transition energies.

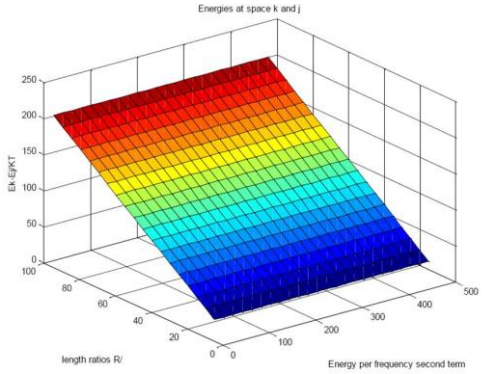

Figure.15 Diagrammatic representation of the term $(\xi_k - \xi_j)/kt$ when $V_o = 1Hz$ and $R > \alpha$ in the second Taylors expansion.

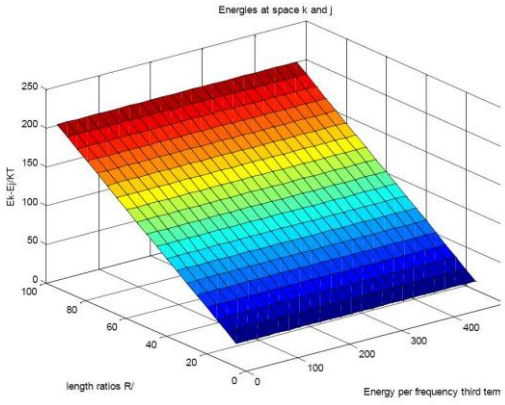

Figure.16 Diagrammatic representation of the term $(\xi_k - \xi_j)/kt$ when $V_o = 1Hz$ and $R > \alpha$ in the general Taylors expansion.

The values for the term $(\xi_k - \xi_j)/kt$ for almost all the simulations were the same. Two figures (15, 16) were highlighted below to explain its features. Figure (15)

describes the effects on the term $(\xi_k - \xi_j)/kt$ when $V_o = 1Hz$ and $R > \alpha$ in the second Taylors expansion. Figure (16) describes the effects on the term $(\xi_k - \xi_j)/kt$ when $V_o = 1Hz$ and $R > \alpha$ in the general Taylors expansion.

RESULTS AND DISCUSSION

Figures (1-4) have the same shape when $R > \alpha$, which shows that beyond the linearity between the localisation length (α) and hopping length (R), the possibility of electron-holes localizing within a site becomes lesser as the attempt-to-escape-frequency (V_0) increases. At this point, the concentration (R) remains constant i.e. 0.2 while the localisation length ranges between 0.0012 and 0.0014. Most importantly, it shows the time dependence of localisation length in a disordered semiconductor. Figures (5, 6) show a different feature. It expresses the effects of the disordered $GaAs - Aa1 - xALAs$ on the localisation length, hopping length and attempt-to-escape-frequency (V_0). The three quantities have the same relations (positive parabolic) to one another with higher magnitudes. This feature in figures (5, 6) simply means that the effect of the localization of the particles on various defects caused by either fluctuations in the well width or by remote charged impurities at increases the calculated lifetime in dependence on the localization length, well width, and other input parameters (Citrin, 1993). Also, increasing the attempt-to-escape frequency, the luminescence lines from the quantum wells are strongly shifted towards higher downward transition energies. Figures (7, 8) are the resultant effect of figures (1, 6). This shows that the indirect recombination time in single quantum wells do not only depend on the applied electric field but on other parameters as hopping distance. The features (shown in figures 9, 14) when $R < \alpha$ revealed strange progression. Figures (9,11,13) whose attempt-to-escape frequency is unity, has a gradual overturn of the shape showing the slow relaxation of quantum particles through a system of localized states which are signatures of transient photoconductivity and optical properties of disordered systems (Monroe, 1985; Takagahara, 1999). When $Vo = 1012Hz$ (figures 10, 12, 14), $GaAs - Aa1 - xALAs$ in particular, experiences an energy relaxation which ultimately depends on the hopping distance. According Baranovskii, Zvyagin, Cordes, Yamasaki, and Thomas (2002) in an exponential density of state, the fastest upwards transitions occur towards a preferred energy level known as the transport energy. Since the hopping transport is governed by upwards transitions from filled states near the Fermi level to empty states (Godet, 2003), we analyzed a balance equilibrium condition (as can be seen in figures (15,16)) where $(\xi_k - \xi_j)/kt = 200$. Secondly, a decrease or increase in the attempt-to-escape frequency had no influence on the $(\xi_k - \xi_j)/kt$. Adopting the experiments of (Golub et al., 1999) where the $GaAs - Aa1 - xALAs$ sample was held in an optical cryostat at temperature $T = 1.4\ K, \xi_k$ and ξ_j which is the energies at each localized state shows an energy splitting between the electronic ground state and the first excited state to be $0.0038eV$.

CONCLUSION

The filling factors of all the energy slices considered are time-dependent and are hence, on equilibrium values. It could be concluded that the distribution of recombining carriers is essentially non equilibrium at low temperatures. We would like to mention that in the system with less disorder, the light emission can be treated using semiconductor Photoluminescence (PL) equation in Eq (10) (Kira, Jahnke, Hoyer, & Koch, 1999). The energy splitting between the electronic ground state and the first excited state ($0.0038eV$) enables the peculiarity of the $GaAs - Aa1 - xALAs$ semiconductor to technological advancement in optoelectronics.

REFERENCE

Ashoori, R., Stormer, H., Weiner, J., Pfeiffer, L., Baldwin, K., & West, K. (1993). N-electron ground state energies of a quantum dot in magnetic field. *Physical Review Letters*, *71*(4), 613-616.

Baranovskii, S., Zvyagin, I., Cordes, H., Yamasaki, S., & Thomas, P. (2002). Electronic transport in disordered organic and inorganic semiconductors. *Journal of non-crystalline solids*, *299*, 416-419.

Citrin, D. (1993). Radiative lifetimes of excitons in quantum wells: Localization and phase-coherence effects. *Physical Review B*, *47*(7), 3832.

Dal Don, B., Kohary, K., Tsitsishvili, E., Kalt, H., Baranovskii, S., & Thomas, P. (2004). Quantitative interpretation of the phonon-assisted redistribution processes of excitons in Zn_ {1-x} Cd_ {x} Se quantum islands. *Physical Review B*, *69*(4), 045318.

Efimkin, D., Kulbachinskii, V., & Lozovik, Y. E. (2011). Influence of disorder on electron-hole pairing in graphene bilayer. *JETP Letters*, *93*(4), 219-222.

Godet, C. (2003). Physics of bandtail hopping in disordered carbons. *Diamond and related materials*, *12*(2), 159-165.

Golub, L., Bookbinder, J., DeLuca, E., Karovska, M., Warren, H., Schrijver, C., . . . Handy, B. (1999). A new view of the solar corona from the transition region and coronal explorer (TRACE). *Physics of Plasmas*, *6*(5), 2205-2216.

Ishibashi, A., Kidoguchi, I., Sugahara, G., & Ban, Y. (2000). High-quality GaN films obtained by air-bridged lateral epitaxial growth. *Journal of crystal growth*, *221*(1), 338-344.

Isu, T., Jiang, D. S., & Ploog, K. (1987). Ultrathin-layer (AlAs) m (GaAs) m superlattices withm= 1, 2, 3 grown by molecular beam epitaxy. *Applied Physics A: Materials Science & Processing*, *43*(1), 75-79.

Kalyanasundaram, K., & Grätzel, M. (1998). Applications of functionalized transition metal complexes in photonic and optoelectronic devices. *Coordination chemistry reviews*, *177*(1), 347-414.

Kira, M., Jahnke, F., Hoyer, W., & Koch, S. (1999). Quantum theory of spontaneous emission and coherent

effects in semiconductor microstructures. *Progress in quantum electronics*, *23*(6), 189-279.

Kramer, B., & MacKinnon, A. (1999). Localization: theory and experiment. *Reports on Progress in Physics*, *56*(12), 1469.

Leadbeater, M., Römer, R. A., & Schreiber, M. (1999). Interaction-dependent enhancement of the localisation length for two interacting particles in a one-dimensional random potential. *The European Physical Journal B-Condensed Matter and Complex Systems*, *8*(4), 643-652.

Marshall, J. (2000). Analytical procedures for the modelling of hopping transport in disordered semiconductors. *Philosophical magazine letters*, *80*(10), 691-701.

Miller, G. L., Blum, R., Glennon, W. E., & Burton, A. L. (1960). Measurement of carboxymethylcellulase activity. *Analytical Biochemistry*, *1*(2), 127-132.

Monroe, D. (1985). Hopping in exponential band tails. *Physical Review Letters*, *54*(2), 146-149.

Ohya, K., Ishida, K., & Mori, I. (1984). Production of Atomic-Oxygen Negative-Ion Beam by Positive Ion-Induced Sputtering of Semiconductive BaTiO3 Ceramic. *Japanese journal of applied physics*, *23*(12), 1640-1646.

Reed, M. A. (1993). Quantum dots. *Scientific American*, *268*(1), 118-123.

Shushin, A. (2011). Magnetic field effects on electron-hole recombination in disordered organic semiconductors. *Physical Review B*, *84*(11), 115212.

Takagahara, T. (1999). Theory of exciton dephasing in semiconductor quantum dots. *Physical Review B*, *60*(4), 2638.